Stress State in Coupling Joints of Posttensioned Concrete Bridges

FRIEDER SEIBLE, YURY KROPP, and CHRISTOPHER T. LATHAM

ABSTRACT

Posttensioned continuous concrete bridges have shown unexpected crack patterns in the vicinity of the theoretical inflection point. In particular, box-girder-type cross sections with coupled posttensioning tendons in construction joints at the points of inflection were found to exhibit an increase in the number and width of cracks in the bottom soffit and webs of the bridge superstructure in the coupling joint vicinity. Intensive investigations attribute these cracks to highly nonlinear stress distributions with significant tensile stress content over the depth of the bridge structure due to nonuniform temperature gradients, concentrated anchorage forces, and increased prestress losses. It is shown that a major factor contributing to the tensile stress potential of the nonlinear stress distribution is a significantly reduced compressive stress state caused by the segmental construction and posttensioning sequence. The uniform state of prestress in a concentrically posttensioned concrete member shows reductions of more than half of the initial prestress in the construction and coupling joint vicinity. Combinations of this reduced compression stress field with prestress losses in the couplers or temperature gradients in the bridge deck show theoretical crack development and crack orientation similar to crack patterns encountered in coupling joint vicinities of posttensioned box-girder bridges.

Large cracks and, in one case, even ruptured tendons found during routine bridge inspections in the Federal Republic of Germany in the vicinity of coupling joints of posttensioned continuous bridge structures (1,2) have led to a series of investigations of the behavior of coupling joints.

Coupling joints of posttensioning tendons are common in segmental bridge construction, particularly in construction methods developed and used frequently in Europe, such as incremental launching and span-by-span erection with traveling self-supporting falsework. It was this latter group of bridge structures that showed crack concentrations in the coupling joint vicinity. In the span-by-span construction method (Figure 1) construction joints with couplers for the tendons are generally placed close to the theoretical point of inflection for dead load plus prestressing to minimize reinforcement requirements in the construction joint. Investigations of crack development in this construction joint vicinity, summarized in Seible (1), showed that initial crack development is caused by several factors such as highly nonlinear stress states due to concentrated anchorage forces, unaccounted differences in the actual dead load distribution, temperature gradients, and increased prestress losses in the tendon couplers. When the section has cracked, the reduction in stiffness, and with it higher cyclic stress levels, must be evaluated carefully because changes in tendon geometry due to the lower strength steel of the anchorage-coupler assembly are cause for stress concentrations and lower fatigue limits (1).

An intensive bridge inspection program by the West German Ministry of Transportation (3) of all bridges with coupling joints revealed the results summarized in Table 1. Two kinds of bridge cross sections are generally used for bridge construction methods that involve coupling joints; namely, box-girders and T-beams with varying numbers of webs and bottom soffit arrangements. Table 1 gives the number of cracked bridge structures encountered, the crack width, and the cracked region for both types of cross section. It can be seen that box-girder sections were found to be more susceptible to cracks in the coupling joint vicinity than T-beam sections, with 30 and 45 percent of the inspected bridge structures showing no cracks, respectively. Cracks wider than one one-hundredth of an inch (>0.2 mm) were more frequently encountered in box-girder sections and, in particular, in the webs and bottom slab. One example of the encountered crack pattern (2) is shown in Figure 2.

The stress states that lead to these cracks, which are parallel and in close proximity to the coupling and construction joint, need to be investigated. It is the purpose of this paper to study in detail the inherent initial stress state of the coupling joint vicinity, due to the various construction and posttensioning stages, and subsequent combinations with possible stress states, due to prestress losses in the coupler or uniform temperature gradients. These stress states explain crack patterns encountered in the coupling joint vicinity and provide the information necessary to properly design these regions.

NONLINEAR STRESS STATES IN COUPLING JOINTS

Nonlinear stress distributions over the depth of a prestressed concrete member can have various causes that range from local force concentrations in the anchorage zones (4,5) to variable temperature gradients (6). A brief summary of these stresses encountered in the coupling joint region is given in this section. Used as an example is a thin-walled, concentrically prestressed concrete member (Figure 3) erected and posttensioned segmentally.

Department of Applied Mechanics and Engineering Sciences, University of California, San Diego, La Jolla, Calif. 92093.

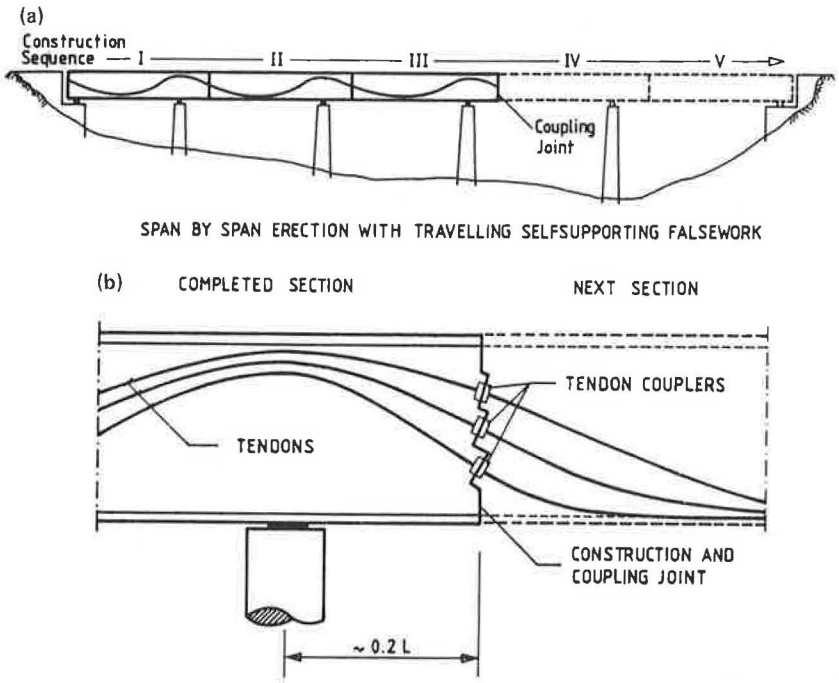

FIGURE 1 Coupling joint: (a) Possible geometry of bridge structure with coupling joints; (b) Coupling joint detail.

Load Conditions Under Investigation

Stress concentrations from tendon anchorages are first present when the initial construction segment is posttensioned and grouted before the formwork is advanced for the construction of the subsequent segment. The stress state is equivalent to the classic case of the infinite half-strip with a concentrated load on the short side (4). To show the accuracy of the chosen linear elastic plane stress model, the splitting stresses are compared with results from Iyengar (5) in Figure 4a normalized with respect to the uniform state of prestress (f_{p0}).

The deformations of the analytical model, which takes advantage of the symmetry in load and geometry along the longitudinal x-axis, are also shown qualitatively in Figures 4a and 4b for the posttensioning of the initial and subsequent segment, denoted as Case 1 and Case 2, respectively.

Additional load cases considered in this study are the time-dependent prying forces, denoted as Case 3, that result from increased prestress losses in the tendon couplers as derived in detail elsewhere (1) and a uniform moment in the plane of the concrete member, denoted as Case 4, that could originate, for example, from the linear portion of a temperature gradient as discussed in Imbsen and Vandershaf (6) or from a shift in the location of the theoretical point of inflection due to self-weight inaccuracies (7) or time-dependent moment redistributions as discussed elsewhere (1). Although both additional load cases (Cases 3 and 4) are time dependent or environmentally dependent, or both, in nature, the actual load intensity factor

TABLE 1 Crack Development in Coupling Joint Vicinity *(2)*

Inspected Bridge Structures									
Cross Section	Total	without cracks	crack width [mm]	with cracks*					
				A	B	C	D	E	F
T-Beam	114 (100%)	51 (45%)	cracked region						
			< 0.2	5	34	2	3	1	0
			> 0.2	2	17	2	2	2	0
Box Girder	184 (100%)	54 (30%)	cracked region						
			< 0.2	5	29	32	5	37	6
			> 0.2	1	4	31	3	54	4

* more than one crack pattern can be encountered in one bridge structure

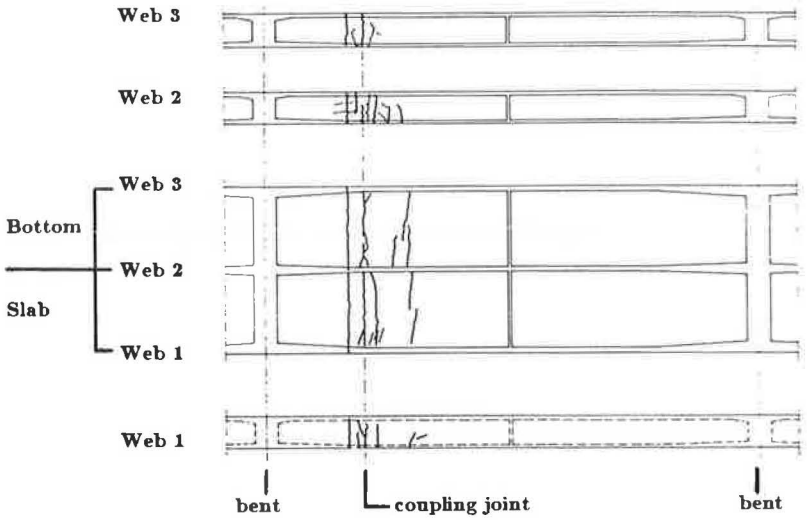

FIGURE 2 Example of crack development in a two-cell box-girder span with coupling joint.

varies for the resulting stress patterns. For Load Case 3, a maximum prying force of 1/2 the initial posttensioning force (P) was selected. This represents a theoretical upper limit for possible prying forces due to increased prestress losses in the tendon coupler as indicated elsewhere (1). The load intensity for Case 4 was chosen to produce maximum tensile extreme fiber stresses of the same magnitude as the uniform prestress (f_{p0}). In the case of a real bridge structure, prestressing levels of f_{p0} = 500 psi (3.5 MN/m^2) are common in the vicinity of the inflection point, and detailed investigations of additional stresses due to temperature differentials, self-weight inaccuracies, and time-dependent force redistributions (8) have shown that actual stress levels of up to 500 psi

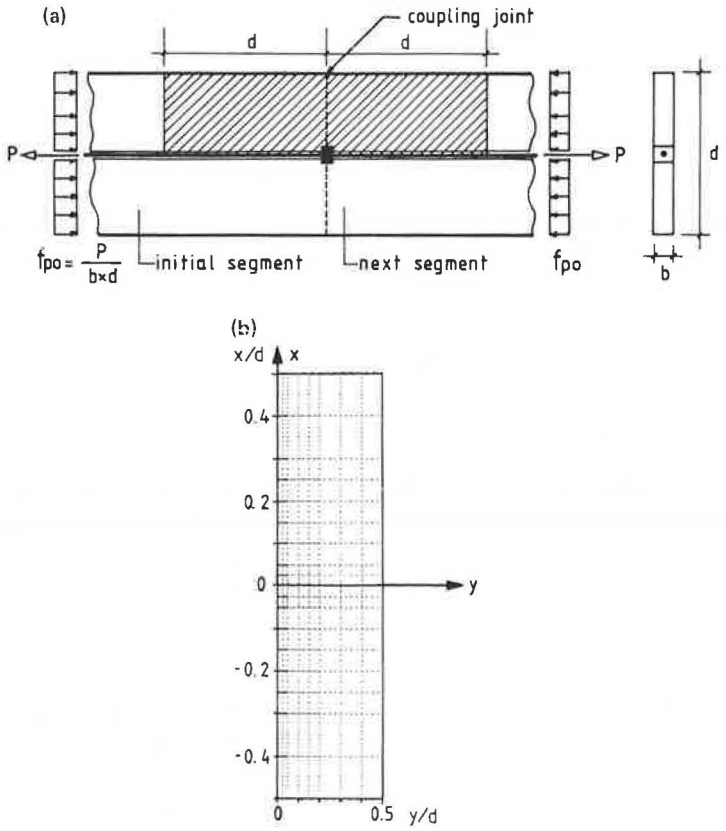

FIGURE 3 Investigated examples: (a) Thin-walled concrete member with single tendon; (b) Analytical model.

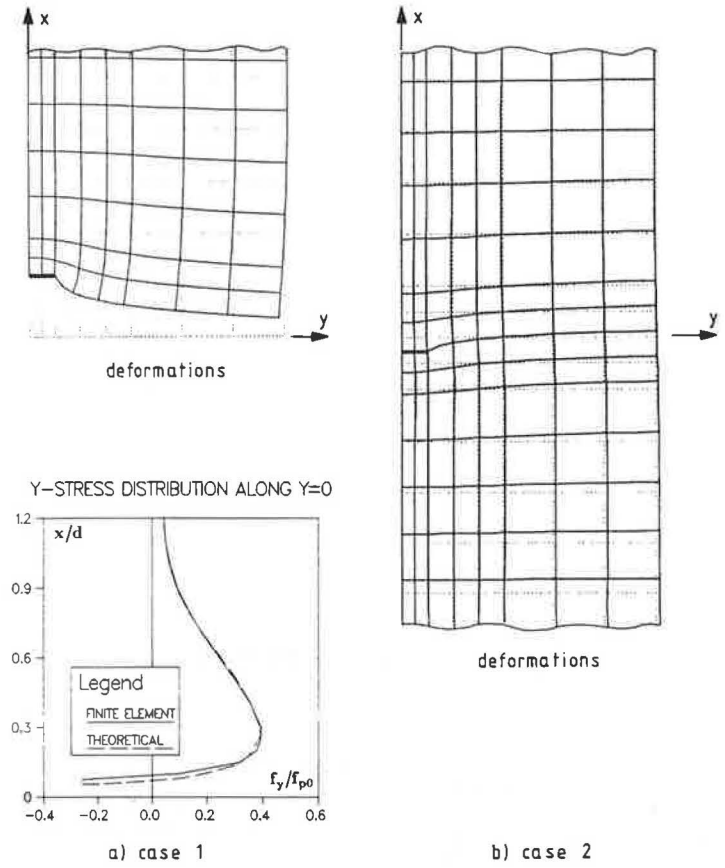

FIGURE 4 Individual construction and posttensioning stages: (a) Deformations and splitting stresses (Case 1); (b) Deformations (Case 2).

(3.5 MN/m^2) are not uncommon in investigated bridge structures. A summary of the individual load conditions is given in Figure 5.

Initial Individual Stress States

Contour plots, shown in Figure 6 for the longitudinal and Figure 7 for the transverse stresses in the coupling joint vicinity, are presented for all four individual load conditions (the construction and posttensioning of the initial segment, the construction and posttensioning of the subsequent segment, the prestress loss in the coupler, and the additional flexural stress state) denoted as Cases 1 through 4, respectively.

Although Case 1 shows the typical stress contour lines for the in-plane distribution of a concentrated edge load and Case 4 shows the trivial pattern for a uniform state of bending, the stress contour lines for Cases 2 and 3 are not so frequently encountered. Of particular interest is the longitudinal stress distribution for the posttensioning of the subsequent segment (Figure 6, Case 2) in which stress levels of 0.5 f_{p0} dominate along the construction joint. This can be attributed to half the posttensioning force for the subsequent segment at the coupling joint being absorbed by the initial segment in the form of a relief stress before direction is reversed in order to satisfy the self-equilibrating applied force state (Figure 6, Case 2).

COMBINATION OF STRESS STATES

The prototype bridge structure experiences a combination of the previously discussed individual stress states. The construction and posttensioning sequence will leave inherent stress states, which deviate substantially from assumed theoretical linear stress distributions of the prestressed concrete structure, in the construction and coupling joint area. Any additional stresses that result from the use of the structure and time or environmentally dependent effects have to be combined with this inherent construction stress state. Because the entire member is subjected to substantial compressive stresses due to prestressing, and because initial cracking during construction can be assumed to be minimized by providing minimum reinforcement for shrinkage, it can be assumed that at low additional load levels the concrete will behave linear elastically, which justifies simple superposition of the previously discussed load and stress patterns.

Inherent Stress State After Segmental Construction

Following the actual construction process of casting, curing, posttensioning (Case 1) and grouting of the initial segment and subsequent casting, curing, and posttensioning (Case 2) of the next segment, the built-in stresses due to the construction sequence are obtained by combining the individual stresses from Cases 1 and 2. The combined stress contour lines (Cases 1 + 2) in the longitudinal and transverse directions are shown in Figure 8.

The longitudinal stress contour plot (x-stress) shows the uniform state of prestress of $f_x/f_{p0} = 1.0$ over most of the investigated area, and deviations occur only in the immediate vicinity ($x/d = \pm 0.4$) of the coupling joint. Large compressive stress con-

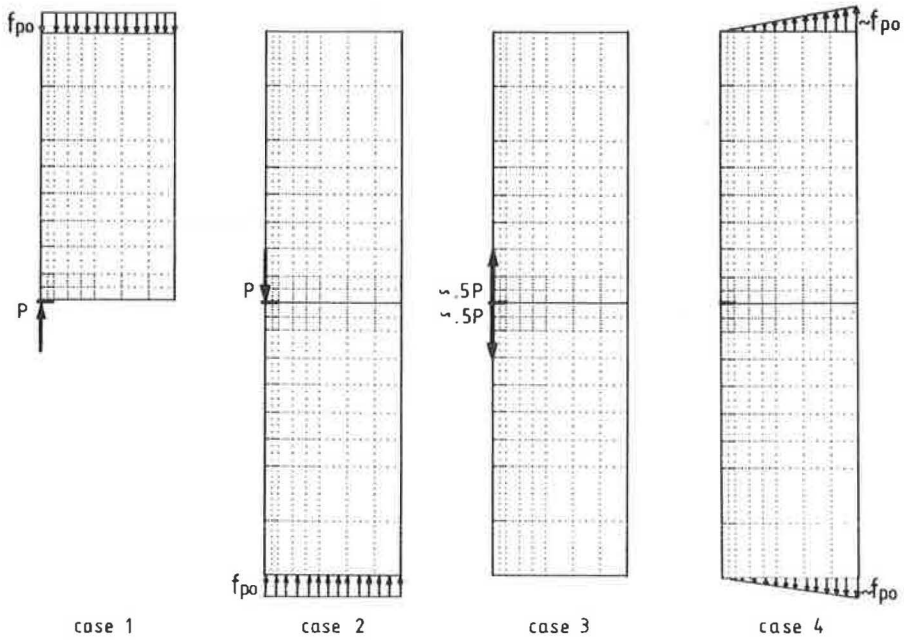

FIGURE 5 Individual load conditions.

centrations are found close to the tendon anchorage or coupler, and a reduced stress state of f_x/f_{p0} = 0.5 prevails over the remaining portion of the construction joint. Of particular interest is a zone at x/d = 0.2 above the construction joint where at the edge of the member a quite localized reduced stress state of f_x/f_{p0} = 0.3 is encountered. If the thin-walled, posttensioned concrete member were prestressed to a uniform 500 psi compressive stress level, Figure 8 indicates that at x/d = 0.2, y/d = 0.5, a compressive stress reserve of only 150 psi would be available immediately after the segmental construction of the member.

To emphasize the longitudinal stress variation in the coupling joint vicinity, Figure 9 shows the x-stresses along selected transverse sections of the thin-walled member. Uniform compressive stress states a distance (x/d = ±0.5) away from the construction joint end, the nonlinear behavior in the direct vicinity of the coupling joint, and the minimum compressive stress reserve at x/d = 0.2, y/d = 0.5 can be clearly identified in Figure 9.

The contour plot of the combined transverse inherent construction stress state (Figure 8, y-stress) shows clearly the critical regions for splitting stresses both in the initial and the subsequent construction segment. It should be noted, however, that the critical splitting stresses in the initial seg-

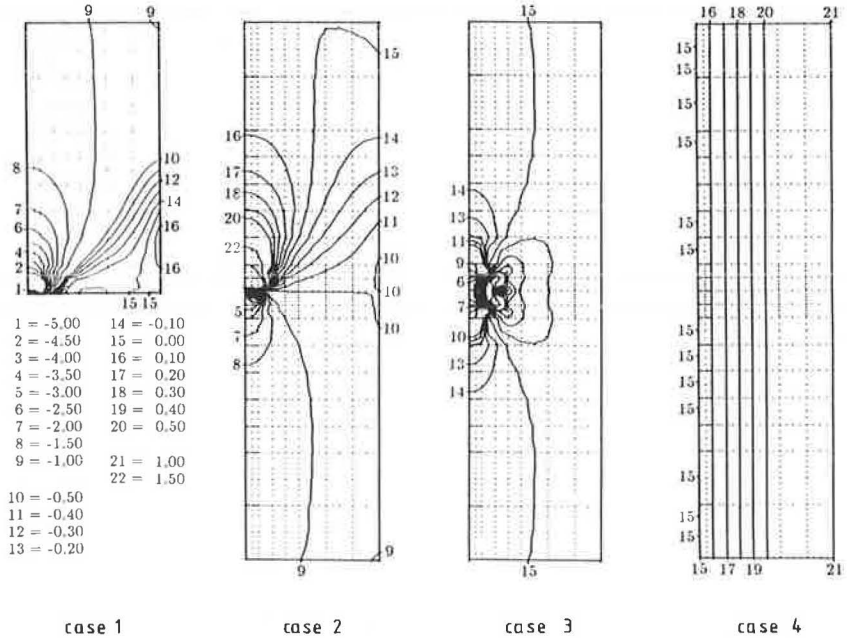

FIGURE 6 Individual longitudinal stress contour lines in coupling joint vicinity.

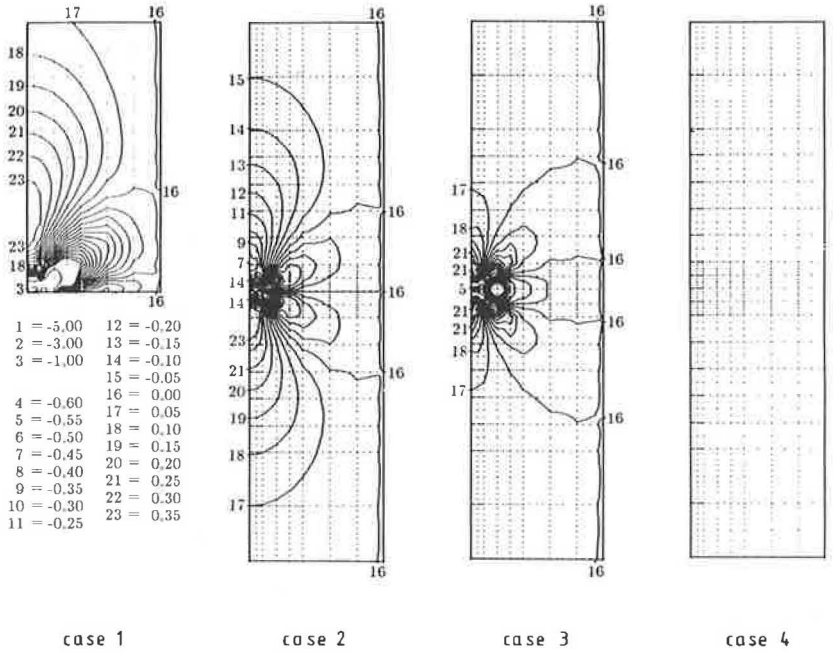

FIGURE 7 Individual transverse stress contour lines in coupling joint vicinity.

ment occur during the posttensioning operation of that segment and are already slightly reduced in Figure 8 by compressive y-stresses from Load Case 2.

Coupled Segments with Possible Losses and Temperature Effects

The longitudinal stress states in the direct coupling joint vicinity for combinations of the inherent construction stress (Cases 1 + 2) with additional stresses resulting from prestress losses in the coupler (Case 3), or additional moments due to temperature differences, or time-dependent shifts in the location of the point of inflection (Case 4) are plotted in Figure 10.

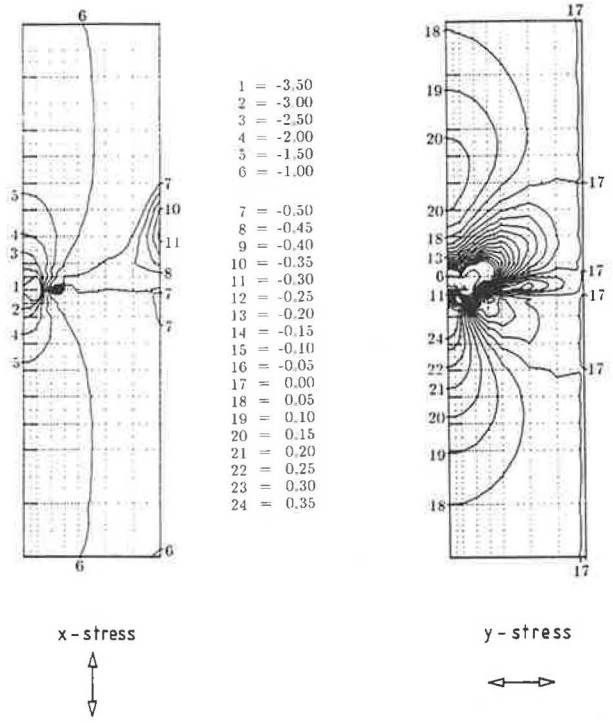

FIGURE 8 Inherent stress contour lines due to construction and posttensioning sequence (Case 1 and 2).

The nonlinear compressive stress reserves from the construction stages (Cases 1 + 2) can be easily exceeded by high local tensile stresses directly adjacent to the tendon coupler (Cases 1 + 2 + 3) and for a wider range at the edge of the member by additional flexural tensile stresses (Cases 1 + 2 + 4). Given these tension zones, the construction joint region can no longer be considered fully prestressed and, depending on the intensity of the superimposed loads, cracks can develop. These cracks in turn will significantly reduce the stiffness of the section in the coupling joint region and thus increase potentially dangerous (9) cyclic stress levels.

CRACK DEVELOPMENT

Crack development in the coupling joint region was traced analytically for the additional Load Cases 3 and 4 starting from the initial inherent construction stress state.

The assumed concrete crack limit was equal in magnitude but opposite in sign to the initial level of prestress f_{p0} (e.g., for the assumed 500-psi compressive state of prestress, the tensile crack limit was also set to 500 psi). The principal stresses were evaluated for each of the element integration points as a combination of the inherent construction stresses and superimposed stresses due to the incremental additional loads. Simplified element stiffness deterioration and crack orientation were determined by a weighted averaging procedure over all element integration points. The direction of crack propagation was found based on the error accumulation method outlined in Pfeiffer et al. (10). In this method the crack is assumed to advance to the one element, of all the elements that have exceeded the cracking stress level, that introduces the least amount of accumulated error as defined by

$$\theta_{error} = \sum_{i=1}^{N} \left(\theta_{L_i} - \theta_{PA_i}\right) \quad (1)$$

$$\theta_{PA_i} = 1/3\left(\theta_{P_{i-1}} + \theta_{P_i} + \theta_{P_{i+1}}\right) \quad (2)$$

where

i = counter of elements along the crack path,
N = number of cracked elements,
θ_{L_i} = angle of the line connecting the ith element with the ith-plus-one element,
θ_{PA_i} = average minimum principal stress direction of three adjacent elements at the ith element, and
θ_{P_i} = direction of minimum principal stress of the ith element.

It should be noted that no stress redistribution of the initial inherent construction stresses was performed because only the crack origination and starting direction, not the complete failure, were investigated.

The two crack patterns for Cases 3 and 4 are shown in Figures 11a and 11b, respectively. Integers from 1 through 4 indicate the order in which elements exceed the cracking stress limit at three or more integration points, and the weighted minimum principal stress directions for these elements are indicated. The final crack patterns, as determined by the pro-

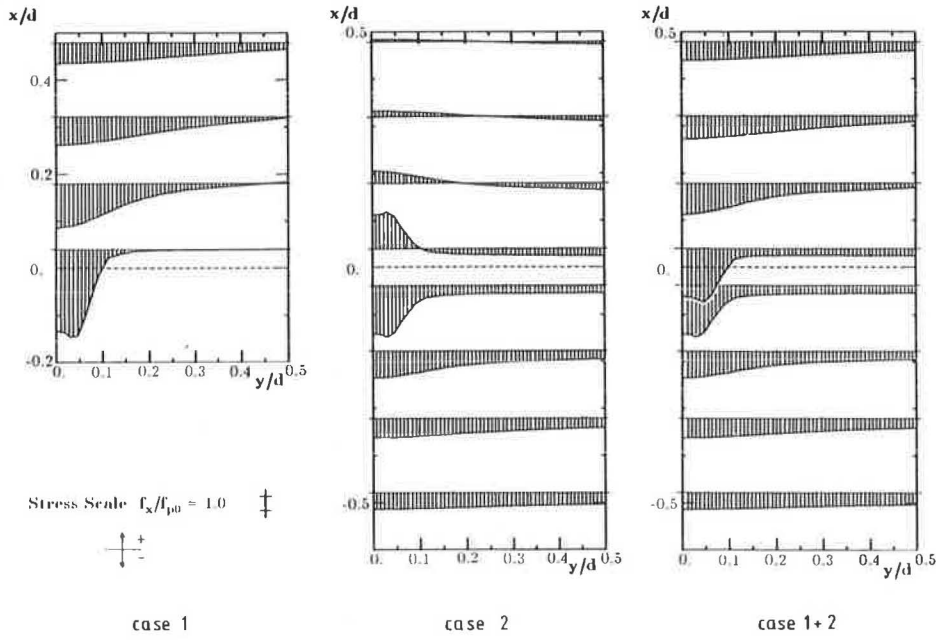

FIGURE 9 Longitudinal stress variations due to construction and posttensioning sequence.

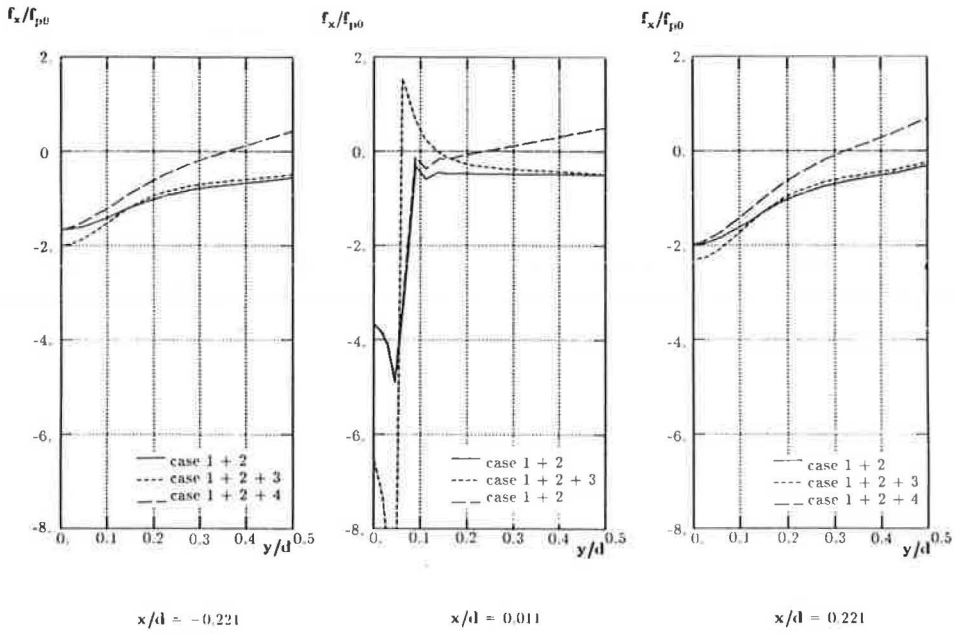

FIGURE 10 Possible longitudinal stress combinations in the construction joint vicinity.

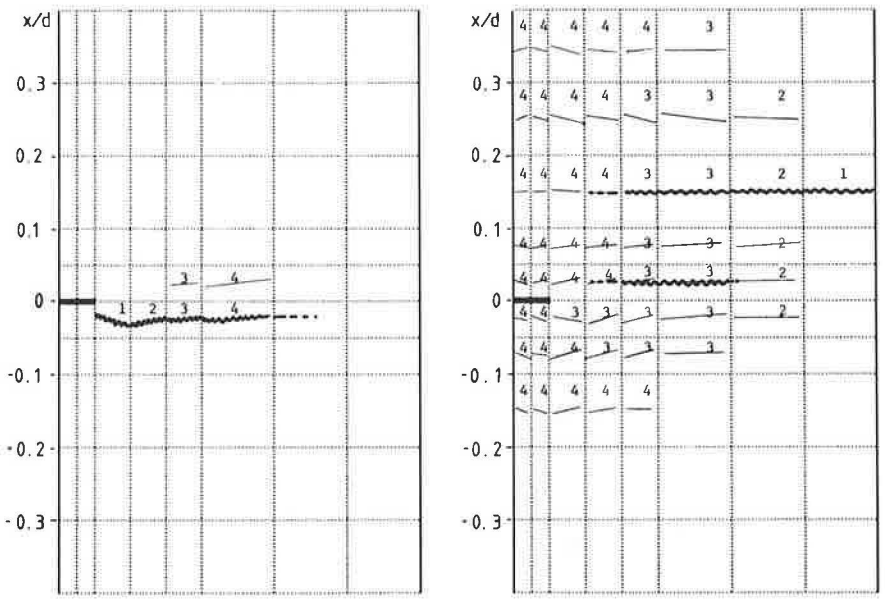

FIGURE 11 Theoretical crack initiation and development.

cedure outlined previously, are shown with bold lines through the cracked elements.

The simplified theoretical crack pattern developments shown in Figure 11 correspond to actual crack patterns encountered in coupling joints of prototype bridge structures with cracks parallel to the construction joint (see Figure 1) and are a direct result of the reduced compressive stress reserves and the nonlinear stress states in the coupling joint region.

CONCLUSIONS AND DESIGN RECOMMENDATIONS

To properly design or evaluate coupling joints of posttensioned concrete members and the direct construction joint vicinity, the following findings from the present investigation should be considered:

- Seemingly uniform compressive stress states of concentrically posttensioned concrete members can be reduced by 50 percent or more in the direct vicinity of the coupling joint as a result of sequential construction and prestressing.
- The same phenomenon applies to eccentrically posttensioned concrete members with one or more coupled tendons with deviations in the expected stress state from the initially assumed linear stress distribution.
- Nonlinear, even though mostly self-equilibrating, local stress states due to increased prestress losses in the coupler or the nonlinear portion of a temperature gradient can quickly exhaust reduced compressive stress capacity and reach cracking levels of the concrete.
- Additional linear stress distribution from linear temperature gradients of unaccounted moments due to creep redistributions or dead load inaccuracies, or both, can also exceed the compressive stress reserves and reduce the section from full to partial prestressing.

General design recommendations, given elsewhere (1), for coupling joints of posttensioned concrete bridges can be formulated more explicitly on the basis of the present findings:

- A simple plane stress investigation of the coupling joint region covering approximately ±d (d = depth of structure) from the construction joint can yield detailed information about the actual compressive stress reserves after segmental construction and posttensioning.
- Additional posttensioning should be provided in this region to reach the minimum design compressive stress levels. If detailed plane stress analysis is not performed, a reduced compressive stress state of 1/2 f_{p0} can be assumed in the coupling joint region.
- Where additional posttensioning of the coupling joint region is not feasible, sufficient regular reinforcement should be provided to cover potential tensile stress regions.
- This additional reinforcement through the construction joint should be provided in the form of closely spaced small-diameter bars to prevent single large cracks from opening and thus preserve structural stiffness and corrosion protection characteristics.

The consequences of cracks in the coupling joint vicinity must be explicitly investigated in the design process to determine cyclic stress levels with respect to reduced fatigue life for built-in anchorage-coupler-tendon assemblies.

REFERENCES

1. F. Seible. Coupling Joints of Prestessing Tendons in Continuous Post-Tensioned Concrete Bridges. In Transportation Research Record 1044, TRB, National Research Council, Washington, D.C., 1985, pp. 43-49.
2. Abteilung Strassenbau, der Bundesminister für Verkehr. Schäden an Brücken und anderen Ingennieurbauwerken. Verkehrsblattverlag Borgmann, Dortmund, Federal Republic of Germany, 1982, 462 pp.
3. Risse in Spannbetonbrücken, insbesondere in Koppelfugenbereichen, Ergebnisse der Risserfassung. B 3.2-3590, Standard vom 31.12.80. Bundesanstalt für Strassenwesen, Bonn, Federal Republic of Germany, June 1981.

4. Y. Guyon. Contraintes dans les pièces prismatiques soumises à des forces appliquées sur leur bases, au voisinage de ces bases. Publications, International Association for Bridges and Structural Engineering, Vol. II, 1951, pp. 165-226.
5. K.T. Sundara Raja Iyengar. Two-Dimensional Theories of Anchorage Zone Stresses in Post-Tensioned Prestressed Beams. Journal of the American Concrete Institute, Proceedings, Vol. 59, No. 10, 1962, pp. 1443-1465.
6. R.A. Imbsen and D.E. Vandershaf. Thermal Effects in Concrete Bridge Superstructures. In Transportation Research Record 950, TRB, National Research Council, Washington, D.C., Vol. 2, 1984, pp. 101-113.
7. G. Koenig and T. Zichner. Berücksichtigung der Temperaturdifferenz ΔT, der Streuung des Eigengewichts und der erhöhten Spannkraftverluste an Spanngliedkopplungen bei der Bemessung Massiver Brücken. Presented at the 8th International Conference of the Féderation Internationale de la Précontrainte, London, England, 1978.
8. W. Rossner. Konstruktion und Bewehrungsführung im Fugenbereich von Brücken bei Abschnittsweiser Herstellung. Beton- und Stahlbetonbau, No. 4, 1981, pp. 89-95.
9. A. Naaman. Prestressed Concrete Analysis and Design, Fundamentals. McGraw-Hill Book Co., New York, 1982, 670 pp.
10. P.A. Pfeiffer, A.H. Marchertas, and Z.P. Bazant. Blunt Crack Band Propogation in Finite Element Analysis for Concrete Structures. 7th International Conference on Structural Mechanics in Reactor Technology, Chicago, Ill., Vol. 5, No. 2, 1983, pp. 227-234.

Publication of this paper sponsored by Committee on General Structures.

Umbrella Loads for Bridge Design

HEINZ P. KORETZKY, KANTILAL R. PATEL, RICHARD M. McCLURE, and DAVID A. VanHORN

ABSTRACT

Recent legislation allowing heavier vehicles on the highway system in Pennsylvania has been assessed for its impact on bridge design. The effect that permit traffic loads and heavy industrial or construction equipment have on bridges has also been assessed. Bending moments for various highway vehicles are illustrated graphically for easy visual comparison. As a result of these studies, Pennsylvania has adopted new umbrella loads for bridge design. The umbrella loads consist of two loads for design purposes (AASHTO HS 25 and 125 percent military) and one load for permit purposes (204,000-lb eight-axle superload).

Described in this paper is the engineering effort that led to replacement of the current AASHTO HS 20 design loading (1) for bridge designs in Pennsylvania with larger loads. Recent legislation allowing heavier vehicles on the state highway system has been assessed for its impact on the umbrella bridge design loads. Various engineering considerations are also outlined including the effect that permit traffic loads and heavy industrial equipment would have on the new design loads. The effect of bending moment for various highway vehicles is illustrated graphically for easy visual comparison.

H.P. Koretzky and K.R. Patel, Pennsylvania Department of Transportation, 1009 Transportation Safety Building, Harrisburg, Pa. 17120. R.M. McClure, Department of Civil Engineering, The Pennsylvania State University, University Park, Pa. 16802. D.A. VanHorn, Department of Civil Engineering, Lehigh University, Bethlehem, Pa. 18015.

PREVIOUS DESIGN LOADINGS

Since 1941 Pennsylvania has used the most conservative AASHTO HS 20 bridge design loading exclusively in the design of every type of state-owned bridge for all classes of highways. This design loading is routinely used by many other states, but some states use the lower class HS 15 loading.

The hypothetical HS loadings are defined in the AASHTO Standard Specifications for Highway Bridges (1). The HS 20 loading is comprised of a single tractor and trailer weighing 36 tons, or an equivalent uniform load with a concentrated load (to simulate a truck train), whichever produces the maximum